# Distributed Cooperative Secondary Control of Microgrids Using Feedback Linearization

Bidram, Ali; Davoudi, Ali; Lewis, Frank; Guerrero, Josep M.

*Published in:*
I E E E Transactions on Power Systems

*DOI (link to publication from Publisher):*
10.1109/TPWRS.2013.2247071

*Publication date:*
2013

*Document Version*
Early version, also known as pre-print

Bidram, A.; Davoudi, A.; Lewis, F.L.; Guerrero, J.M., "Distributed Cooperative Secondary Control of Microgrids Using Feedback Linearization," *Power Systems, IEEE Transactions on* , vol.PP, no.99, pp.1-9, 2013.
URL: http://ieeexplore.ieee.org/stamp/stamp.jsp?tp=&arnumber=6475213&isnumber=4374138

# Distributed Cooperative Secondary Control of Microgrids Using Feedback Linearization

Ali Bidram, *Graduate Student Member, IEEE*, Ali Davoudi, *Member, IEEE*, Frank L. Lewis, *Fellow, IEEE*, and Josep M. Guerrero, *Senior Member, IEEE*

***Abstract*— This paper proposes a secondary voltage control of microgrids based on the distributed cooperative control of multi-agent systems. The proposed secondary control is fully distributed; each distributed generator (DG) only requires its own information and the information of some neighbors. The distributed structure obviates the requirements for a central controller and complex communication network which, in turn, improves the system reliability. Input-output feedback linearization is used to convert the secondary voltage control to a linear second-order tracker synchronization problem. The control parameters can be tuned to obtain a desired response speed. The effectiveness of the proposed control methodology is verified by the simulation of a microgrid test system.**

***Index Terms*—Distributed generator, distributed cooperative control, feedback linearization, microgrid, multi-agent systems, secondary control.**

## I. Introduction

The electric power system is experiencing a rapid transformation to an intelligent electric network, the so-called smart gird. Microgrids, as the building blocks of smart grids, are small-scale power systems that facilitate the effective integration of distributed generators (DG) [1]-[3]. Proper control of microgrids is a prerequisite for stable and economically efficient operations of smart grids [5]-[6]. Microgrids can operate in both grid-connected and islanded operating modes.

In normal operation, the microgrid is connected to the main grid. In the event of a disturbance, the microgrid disconnects from the main grid and enters the islanded operation. Once a microgrid is islanded, the so-called primary control maintains the voltage and frequency stability [6]-[10]. However, even in the presence of primary control, voltage and frequency can still deviate from their nominal values. To restore the voltage and frequency of DGs to their nominal values, the so-called secondary control is also required [6]-[7], [11]-[18].

Conventional secondary controls of microgrids assume a centralized control structure that requires a complex communication network [6], [7], [12], in some cases, with two-way communication links [11]. This can adversely affect the system reliability. Alternatively, distributed cooperative control structures, with sparse communication network, are suitable alternatives for the secondary control of microgrids. Distributed cooperative control is recently introduced in power systems [19], to regulate the output power of multiple photovoltaic generators.

Over the last two decades, networked multi-agent systems have earned much attention due to their flexibility and computational efficiency. These systems are inspired by the natural phenomena such as swarming in insects, flocking in birds, thermodynamics laws, and synchronization and phase transitions in physical and chemical systems. In these phenomena, the coordination and synchronization process necessitates that each agent exchange information with other agents according to some restricted communication protocols [20]-[23].

In this paper, distributed cooperative control of multi-agent systems is adopted to implement the secondary control of microgirds. The term “distributed” means that the controller requires a communication network by which each agent only receives the information of its neighboring agents. The term “cooperative” means that, in contrast to the competitive control, all agents act as one group towards a common synchronization goal and follow cooperative decisions [20]-[24]. Distributed cooperative control of multi-agent systems is mainly categorized into the regulator synchronization problem and the tracking synchronization problem. In regulator synchronization problem, also called leaderless consensus, all agents synchronize to a common value that is not prescribed or controllable. In tracking synchronization problem, all agents synchronize to a leader node that acts as a command generator [25]-[27]. Neighboring agents can communicate with each other. The leader is only connected to a small portion of the agents [25].

Distributed cooperative control for multi-agent systems with nonlinear or non-identical dynamics has been recently introduced in the literature [26]-[28]. Considering DGs in a microgrid as agents in a networked multi-agent system, the secondary control design resembles a tracking synchronization problem. The dynamics of DGs in microgrids are nonlinear and

This work was supported in part by the NSF under Grant Numbers ECCS-1137354 and ECCS-1128050, by the AFOSR under Grant Number FA9550-09-1-0278, by the ARO under Grant Number W91NF-05-1-0314, and by the China NNSF under Grant Number 61120106011.

A. Bidram, A. Davoudi, and F. L. Lewis are with the University of Texas at Arlington Research Institute, University of Texas at Arlington, 7300 Jack Newell Blvd. S., Ft. Worth, TX 76118 USA (e-mail: ali.bidram@mavs.uta.edu; davoudi@uta.edu; lewis@uta.edu). J. M. Guerrero is with the Department of Energy Technology, Aalborg University, 9220 Aalborg East, Denmark (Tel: +45 2037 8262; Fax: +45 9815 1411; e-mail: joz@et.aau.dk).

non-identical; input-output feedback linearization is used to transform the nonlinear heterogeneous dynamics of DGs to linear dynamics. Thus, the secondary voltage control is transformed to a second-order tracking synchronization problem. The Lyapunov technique is then adopted to derive fully distributed control protocols for each DG.

In this paper, the distributed cooperative control of multi-agent systems is used to design the secondary voltage control of a microgrid system. The salient features of the proposed control methodology are:

- The secondary voltage control of microgrids is implemented using the concept of distributed cooperative control of multi-agent systems.
- Input-output feedback linearization is used to solve the tracking synchronization problem for nonlinear and heterogeneous multi-agent systems.
- The proposed secondary voltage control obviates the requirement for a central controller and requires only a sparse communication structure with one-way communication links which is cheaper and can be more reliable.
- Desired response speeds can be obtained by tuning the control parameters.

This paper is organized as follows: Section II discusses the primary and secondary control levels. In Section III, the dynamical model of inverter-based DGs is presented. In Section IV, input-output feedback linearization is adopted to design a secondary voltage control based on distributed cooperative control. The proposed secondary control is verified in section V using a microgrid test system. Section VI concludes the paper.

## II. Microgrid Primary and Secondary Control Levels

A microgrid is able to operate in both grid-connected and islanded modes. The voltage and frequency of the microgrid in the grid-connected mode are dictated by the main grid [6]-[7]. The microgrid can switch to the islanded mode due to the preplanned scheduling or unplanned disturbances. Subsequent to the islanding process, the primary control [6]-[10] maintains the voltage and frequency stability of the microgrid. Primary control avoids voltage and frequency instability by keeping these values in pre-specified ranges. However, it might not return the microgrid to the normal operating conditions and an additional control level is required to restore the voltage and frequency. This functionality is provided by the secondary control, which compensates for the voltage and frequency deviations caused by the primary control [6]-[7]. The secondary control operates with a longer time frame than primary control [12]. This facilitates the decoupled operation and design of primary and secondary control levels.

Primary control is usually implemented as a local controller at each DG. This control level always exists and takes action in the event of disturbances. Coordinated control of the primary local controllers can be achieved by the active and reactive-power droop techniques [6]-[7]. Droop technique prescribes a desired relation between the frequency and active power $P$, and between the voltage amplitude and reactive power $Q$. The frequency and voltage droop characteristics for the $i^{\text{th}}$ DG are given by

$$\omega_i = \omega_{ni} - m_{Pi} P_i, \tag{1}$$

$$v^*_{o,magi} = V_{ni} - n_{Qi} Q_i. \tag{2}$$

where $v^*_{o,magi}$ is the reference value for the output voltage magnitude that is provided for the internal voltage control loop of DG. $\omega_i$ is the angular frequency of the DG dictated by the primary control. $P_i$ and $Q_i$ are the measured active and reactive power at the DG's terminal. $m_{Pi}$ and $n_{Qi}$ are the droop coefficients. $V_{ni}$ and $\omega_{ni}$ are the primary control references [6]-[7]. The droop coefficients are selected based on the active and reactive power ratings of each DG.

The secondary control sets the references for the primary control, $V_{ni}$ and $\omega_{ni}$ in (1), so as to regulate the frequency and voltage amplitude to their prescribed nominal values. Conventionally, the secondary control is implemented for each DG using a centralized controller having the proportional-plus-integral (PI) structure [6]-[7]. This secondary control is centralized and requires a star communication structure. In a star communication structure, it is necessary to have a communication link between all DGs and the central controller. Due to the centralized structure of this controller, this control scheme can potentially be unreliable. Alternatively, a distributed cooperative control structure is proposed in this paper.

## III. Large-signal Dynamical Model of Inverter-based Distributed Generators

The proposed secondary voltage control is designed based on the large-signal nonlinear dynamical model of the DG. The block diagram of an inverter-based DG is shown in Fig. 1. It contains an inverter bridge, connected to a primary dc power source (e.g., photovoltaic panels or fuel cells). The control loops, including the power, voltage, and current controllers, adjust the output voltage and frequency of the inverter bridge [29]-[31]. Given the relatively high switching frequency of the inverter bridge, the switching artifacts can be safely neglected via average-value modeling. As stated in [29], dc-bus dynamics can be safely neglected, assuming an ideal source from the DG side.

It should be noted that the nonlinear dynamics of each DG are formulated in its own *d-q* (direct-quadrature) reference frame. It is assumed that the reference frame of the $i^{\text{th}}$ DG is rotating at the frequency of $\omega_i$. The reference frame of one DG is considered as the common reference frame with the rotating frequency of $\omega_{com}$. The angle of the $i^{\text{th}}$ DG reference frame, with respect to the common reference frame, is denoted as $\delta_i$ and satisfies the following differential equation

$$\dot{\delta}_i = \omega_i - \omega_{com}. \tag{3}$$

Although different angular frequencies are considered for reference frames, all the reference frames rotate synchronously at a common angular frequency due to the presence of the frequency-droop characteristic in (1).

The power controller block, shown in Fig. 2, contains the droop technique in (1), and provides the voltage references $v^*_{odi}$ and $v^*_{oqi}$ for the voltage controller, as well as the operating frequency $\omega_i$ for the inverter bridge. Two low-pass filters with the cut-off frequency of $\omega_{ci}$ are used to extract the fundamental component of the output active and reactive powers, denoted as $P_i$ and $Q_i$, respectively. The differential equations of the power controller can be written as

$$\dot{P}_i = -\omega_{ci} P_i + \omega_{ci}(v_{odi} i_{odi} + v_{oqi} i_{oqi}), \tag{4}$$

$$\dot{Q}_i = -\omega_{ci} Q_i + \omega_{ci}(v_{oqi} i_{odi} - v_{odi} i_{oqi}). \tag{5}$$

where $v_{odi}$, $v_{oqi}$, $i_{odi}$, and $i_{oqi}$ are the direct and quadrature components of $v_{oi}$ and $i_{oi}$ in Fig. 1. As seen in Fig. 2, the primary voltage control strategy for each DG aligns the output voltage magnitude on the d-axis of the corresponding reference frame. Therefore

$$\begin{cases} v^*_{odi} = V_{ni} - n_{Qi} Q_i \\ v^*_{oqi} = 0 \end{cases}. \tag{6}$$

The block diagram of the voltage controller is shown in Fig. 3 [30]-[31]. The differential algebraic equations of the voltage controller are written as

$$\dot{\phi}_{di} = v^*_{odi} - v_{odi}, \tag{7}$$

$$\dot{\phi}_{qi} = v^*_{oqi} - v_{oqi}, \tag{8}$$

$$i^*_{ldi} = F_i i_{odi} - \omega_b C_{fi} v_{oqi} + K_{PVi}(v^*_{odi} - v_{odi}) + K_{IVi}\phi_{di}, \tag{9}$$

$$i^*_{lqi} = F_i i_{oqi} + \omega_b C_{fi} v_{odi} + K_{PVi}(v^*_{oqi} - v_{oqi}) + K_{IVi}\phi_{qi}, \tag{10}$$

where $\phi_{di}$ and $\phi_{qi}$ are the auxiliary state variables defined for PI controllers in Fig. 3. $\omega_b$ is the nominal angular frequency. Other parameters are shown in Figs. 1 and 3.

The block diagram of the current controller is shown in Fig. 4 [30]-[31]. The differential algebraic equations of the current controller are written as

$$\dot{\gamma}_{di} = i^*_{ldi} - i_{ldi}, \tag{11}$$

$$\dot{\gamma}_{qi} = i^*_{lqi} - i_{lqi}, \tag{12}$$

$$v^*_{idi} = -\omega_b L_{fi} i_{lqi} + K_{PCi}(i^*_{ldi} - i_{ldi}) + K_{ICi}\gamma_{di}, \tag{13}$$

$$v^*_{iqi} = \omega_b L_{fi} i_{ldi} + K_{PCi}(i^*_{lqi} - i_{lqi}) + K_{ICi}\gamma_{qi}, \tag{14}$$

where $\gamma_{di}$ and $\gamma_{qi}$ are the auxiliary state variables defined for the PI controllers in Fig. 4. $i_{ldi}$ and $i_{lqi}$ are the direct and quadrature components of $i_{li}$ in Fig. 1. Other parameters are shown in Figs. 1 and 4.

The differential equations for the output LC filter and output connector are as follows.

$$\dot{i}_{ldi} = -\frac{R_{fi}}{L_{fi}} i_{ldi} + \omega_i i_{lqi} + \frac{1}{L_{fi}} v_{idi} - \frac{1}{L_{fi}} v_{odi}, \tag{15}$$

$$\dot{i}_{lqi} = -\frac{R_{fi}}{L_{fi}} i_{lqi} - \omega_i i_{ldi} + \frac{1}{L_{fi}} v_{iqi} - \frac{1}{L_{fi}} v_{oqi}, \tag{16}$$

$$\dot{v}_{odi} = \omega_i v_{oqi} + \frac{1}{C_{fi}} i_{ldi} - \frac{1}{C_{fi}} i_{odi}, \tag{17}$$

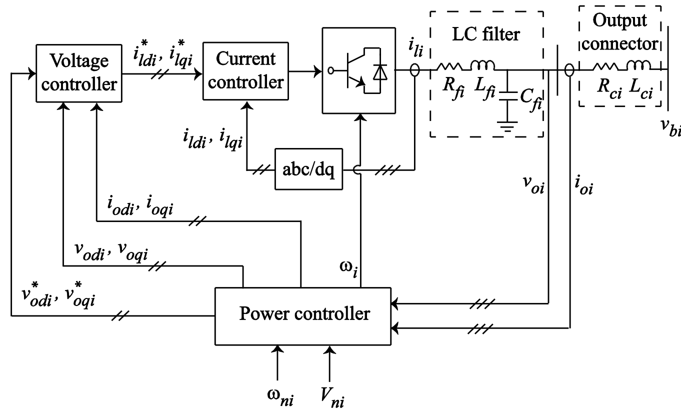


Fig. 1. The block diagram of an inverter-based DG.

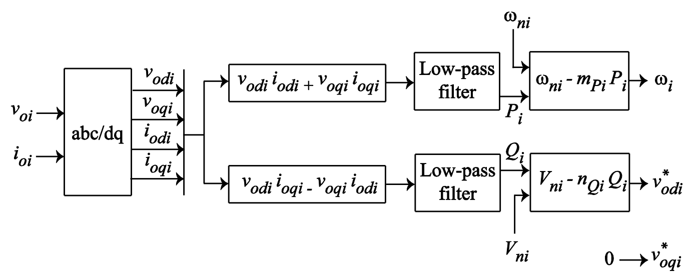


Fig. 2. The block diagram of the power controller.

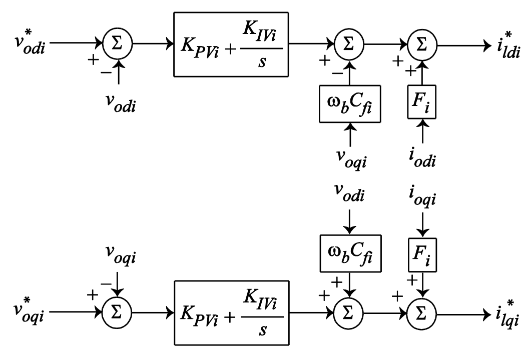


Fig. 3. The block diagram of the voltage controller.

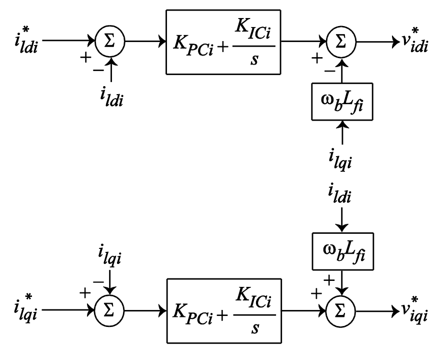


Fig. 4. The block diagram of the current controller.

$$\dot{v}_{oqi} = -\omega_i v_{odi} + \frac{1}{C_{fi}} i_{lqi} - \frac{1}{C_{fi}} i_{oqi}, \tag{18}$$

$$\dot{i}_{odi} = -\frac{R_{ci}}{L_{ci}} i_{odi} + \omega_i i_{oqi} + \frac{1}{L_{ci}} v_{odi} - \frac{1}{L_{ci}} v_{bdi}, \tag{19}$$

$$\dot{i}_{oqi} = -\frac{R_{ci}}{L_{ci}} i_{oqi} - \omega_i i_{odi} + \frac{1}{L_{ci}} v_{oqi} - \frac{1}{L_{ci}} v_{bqi}. \tag{20}$$

Equations (3)-(20) form the large-signal dynamical model of the $i^{th}$ DG. The large-signal dynamical model can be written in a compact form as

$$\begin{cases} \dot{\mathbf{x}}_i = \mathbf{f}_i(\mathbf{x}_i) + \mathbf{k}_i(\mathbf{x}_i)\mathbf{D}_i + \mathbf{g}_i(\mathbf{x}_i)u_i \\ y_i = h_i(\mathbf{x}_i) \end{cases}, \tag{21}$$

where the state vector is

$$\mathbf{x}_i = [\delta_i \quad P_i \quad Q_i \quad \phi_{di} \quad \phi_{qi} \quad \gamma_{di} \quad \gamma_{qi} \quad i_{ldi} \quad i_{lqi} \quad v_{odi} \quad v_{oqi} \quad i_{odi} \quad i_{oqi}]^T. \tag{22}$$

The term $\mathbf{D}_i=[\omega_{com} \ v_{bdi} \ v_{bqi}]^T$ is considered as a known disturbance. The detailed expressions for $\mathbf{f}_i(\mathbf{x}_i)$, $\mathbf{g}_i(\mathbf{x}_i)$, and $\mathbf{k}_i(\mathbf{x}_i)$ can be extracted from (3) to (20).

The secondary voltage control selects $V_{ni}$ in (1) such that the terminal voltage amplitude of each DG approaches its nominal value, i.e. $v_{o,magi} \rightarrow v_{ref}$. Since the amplitude of the DG output voltage is

$$v_{o,magi} = \sqrt{{v_{odi}}^2 + {v_{oqi}}^2}, \tag{23}$$

the synchronization of the voltage amplitude can be achieved by choosing the control input $V_{ni}$ such that $v_{odi} \rightarrow v_{ref}$. Therefore, for the secondary voltage control, the output and control input are set to $y_i=v_{odi}$ and $u_i=V_{ni}$, respectively.

## IV. Secondary Voltage Control Based on Distributed Cooperative Control

A microgrid resembles a nonlinear and heterogeneous multi-agent system, where each DG is an agent. The secondary control of microgrids is a tracking synchronization problem, where all DGs try to synchronize their terminal voltage amplitude to pre-specified reference values. For this purpose, each DG needs to communicate with its neighbors only. The required communication network can be modeled by a communication graph.

In this section, first, a preliminary on the graph theory is presented. Then, the secondary voltage control is implemented through input-output feedback linearization and distributed cooperative control of multi-agent systems. Finally, the communication network requirements for the proposed secondary voltage control are discussed.

### *A. Preliminary of Graph Theory*

The communication network of a multi-agent cooperative system can be modeled by a directed graph (digraph). A digraph is usually expressed as $Gr=(V_G,E_G,A_G)$ with a nonempty finite set of $N$ nodes $V_G=\{v_1,v_2,\ldots,v_N\}$, a set of edges or arcs $E_G \subset V_G \times V_G$, and the associated adjacency matrix $A_G=[a_{ij}] \in R^{N\times N}$. In a microgrid, DGs are considered as the nodes of the communication digraph. The edges of the corresponding digraph of the communication network denote the communication links.

In this paper, the digraph is assumed to be time invariant, i.e., $A_G$ is constant. An edge from node $j$ to node $i$ is denoted by $(v_j,v_i)$, which means that node $i$ receives the information from node $j$. $a_{ij}$ is the weight of edge $(v_j,v_i)$, and $a_{ij}>0$ if $(v_j,v_i) \in E_G$, otherwise $a_{ij}=0$. Node $i$ is called a neighbor of node $j$ if $(v_i,v_j) \in E_G$. The set of neighbors of node $j$ is denoted as $N_j=\{i \,|\, (v_i,v_j) \in E_G\}$. For a digraph, if node $i$ is a neighbor of node $j$, then node $j$ can get information from node $i$, but not necessarily vice versa. The in-degree matrix is defined as $D=diag\{d_i\} \in R^{N\times N}$ with $d_i = \sum_{j\in N_i} a_{ij}$. The Laplacian matrix is defined as $L=D-A_G$. A direct path from node $i$ to node $j$ is a sequence of edges, expressed as $\{(v_i,v_k),(v_k,v_l),\ldots,(v_m,v_j)\}$. A digraph is said to have a spanning tree, if there is a root node with a direct path from that node to every other node in the graph [24].

### *B. Cooperative Secondary Voltage Control Based on Feedback Linearization and Tracking Synchronization Problem*

As discussed in Section III, the secondary voltage control chooses appropriate control inputs $V_{ni}$ in (1) to synchronize the voltage magnitudes of DGs $v_{o,magi}$ to the reference voltage $v_{ref}$. The synchronization of the voltage magnitudes of DGs, $v_{o,magi}$, is equivalent to synchronizing the direct term of output voltages $v_{odi}$. Therefore, the secondary voltage control should choose $u_i$ in (21) such that $y_i \rightarrow y_0$, $\forall i$, where $y_0 \equiv v_{ref}$.

Since the dynamics of DGs in a microgrid are nonlinear and might not be all identical, input-output feedback linearization can be used to facilitate the secondary voltage control design. In input-output feedback linearization, a direct relationship between the dynamics of the output $y_i$ (or equivalently $v_{odi}$) and the control input $u_i$ (or equivalently $V_{ni}$) is generated by repetitively differentiating $y_i$ with respect to time.

For the dynamics of the $i^{th}$ DG in (21), the direct relationship between the $y_i$ and $u_i$ is generated after the $2^{nd}$ derivative of the output $y_i$

$$\ddot{y}_i = {L_{\mathbf{F}_i}}^2 h_i + L_{\mathbf{g}_i} L_{\mathbf{F}_i} h_i u_i, \tag{24}$$

where

$$\mathbf{F}_i(\mathbf{x}_i) = \mathbf{f}_i(\mathbf{x}_i) + \mathbf{k}_i(\mathbf{x}_i)\mathbf{D}_i. \tag{25}$$

$L_{\mathbf{F}_i} h_i$ is the Lie derivative [32] of $h_i$ with respect to $\mathbf{F}_i$, and is defined by $L_{\mathbf{F}_i} h_i = \nabla h_i \mathbf{F}_i = \dfrac{\partial(h_i)}{\partial \mathbf{x}_i}\mathbf{F}_i$. ${L_{\mathbf{F}_i}}^2 h_i$ is defined by ${L_{\mathbf{F}_i}}^2 h_i = L_{\mathbf{F}_i}(L_{\mathbf{F}_i} h_i) = \dfrac{\partial(L_{\mathbf{F}_i} h_i)}{\partial \mathbf{x}_i}\mathbf{F}_i$.

An auxiliary control $v_i$ is defined as

$$v_i = {L_{\mathbf{F}_i}}^2 h_i + L_{\mathbf{g}_i} L_{\mathbf{F}_i} h_i u_i. \tag{26}$$

Equations (24) and (26) result in the $2^{nd}$-order linear system

$$\ddot{y}_i = v_i, \forall i. \tag{27}$$

By choosing appropriate $v_i$, the synchronization for $y_i$ is provided. The control input $u_i$ is implemented by $v_i$ as

$$u_i = (L_{\mathbf{g}_i} L_{\mathbf{F}_i} h_i)^{-1}(-{L_{\mathbf{F}_i}}^2 h_i + v_i). \tag{28}$$

In the following, the procedure for designing appropriate $v_i$ is elaborated. First, equation (27) and the first derivative of $y_i$ are written as

$$\begin{cases} \dot{y}_i \equiv y_{i,1} \\ \dot{y}_{i,1} = v_i \end{cases}, \forall i. \tag{29}$$

or equivalently

$$\dot{\mathbf{y}}_i = \mathbf{A}\mathbf{y}_i + \mathbf{B}v_i, \forall i. \tag{30}$$

where $\mathbf{y}_i = [y_i \quad y_{i,1}]^T$, $\mathbf{B} = [0 \quad 1]^T$, and $\mathbf{A} = \begin{bmatrix} 0 & 1 \\ 0 & 0 \end{bmatrix}$.

Using input-output feedback linearization, the nonlinear dynamics of each DG in (21) are transformed to (30) and a set of internal dynamics. The commensurate reformulated dynamics of the reference generator can be expressed as

$$\dot{\mathbf{y}}_0 = \mathbf{A}\mathbf{y}_0, \tag{31}$$

where $\mathbf{y}_0 = [y_0 \quad \dot{y}_0]^T$. It should be noted that since $y_0 = v_{ref}$ is constant, $\dot{y}_0 = 0$.

It is assumed that DGs can communicate with each other through a communication network described by the digraph $Gr$. Based on the digraph $Gr$, the $i^{\text{th}}$ DG may need to transmit $\mathbf{y}_i$ in (30) through the communication network. It is assumed that only one DG has the access to the reference $\mathbf{y}_0$ in (31) by a weight factor known as the pinning gain $g_i$. The secondary voltage control problem is to find a distributed $v_i$ in (28) such that $\mathbf{y}_i \to \mathbf{y}_0$, $\forall i$. To solve this problem, the cooperative team objectives are expressed in terms of the local neighborhood tracking error

$$\mathbf{e}_i = \sum_{j \in N_i} a_{ij}(\mathbf{y}_i - \mathbf{y}_j) + g_i(\mathbf{y}_i - \mathbf{y}_0), \tag{32}$$

where $a_{ij}$ denotes the elements of the communication digraph adjacency matrix. The pinning gain $g_i$ is nonzero for one DG.

For a microgrid including $N$ DGs, the global error vector for graph $Gr$ is written from (32) as [24]

$$\mathbf{e} = \big((L+G)\otimes I_2\big)(\mathbf{Y} - \mathbf{Y}_0) \equiv \big((L+G)\otimes I_2\big)\boldsymbol{\delta}, \tag{33}$$

where $\mathbf{Y}=[\mathbf{y}_1^T\ \mathbf{y}_2^T\ ...\ \mathbf{y}_N^T]^T$, $\mathbf{e}=[\mathbf{e}_1^T\ \mathbf{e}_2^T\ ...\ \mathbf{e}_N^T]^T$, $\mathbf{Y}_0=\mathbf{1}_N\mathbf{y}_0$ ($\mathbf{1}_N$ is the vector of ones with the length of $N$.), $G=diag\{g_i\}$, $I_2$ is the identity matrix with 2 rows and two columns, and $\boldsymbol{\delta}$ is the global disagreement vector. The Kronecker product is shown as $\otimes$[33]. $\dot{\mathbf{Y}}$ can be written as

$$\dot{\mathbf{Y}} = (I_N \otimes \mathbf{A})\mathbf{Y} + (I_N \otimes \mathbf{B})\mathbf{v}, \tag{34}$$

Where $\mathbf{v}=[v_1\, v_2 \ldots v_N]^T$ is the global auxiliary control vector. $\dot{\mathbf{Y}}_0$ can be written as

$$\dot{\mathbf{Y}}_0 = (I_N \otimes \mathbf{A})\mathbf{Y}_0. \tag{35}$$

The following definitions and lemmas are required for designing the auxiliary controls $v_i$.

*Definition 1* [34]. ($\mathbf{A}$,$\mathbf{B}$) are stabilizable if there exists a matrix $S$ such that all eigenvalues of $\mathbf{A}$-$\mathbf{B}S$ have a strictly-negative real part.

*Definition 2* [34]. A matrix is Hurwitz if all of its eigenvalues have a strictly-negative real part.

*Definition 3* [34]. A symmetric matrix $P$ is positive definite if $x^TPx$ is positive for all non-zero column vector $x$, and $x^TPx$ is zero only for $x$=0.

*Lemma 1* [22], [35]. Let ($\mathbf{A}$,$\mathbf{B}$) be stabilizable**.** Let the digraph $Gr$ have a spanning tree and $g_i \neq 0$ for one DG placed on a root node of the digraph $Gr$. Let $\lambda_i$ ($i \in \{1,2,\ldots,\text{N}\}$) be the eigenvalues of $L$+$G$. The matrix

$$\mathbf{H} = I_N \otimes \mathbf{A} - c(L+G)\otimes \mathbf{B}K, \tag{36}$$

with $c \in R$ and $K \in R^{1\times 2}$, is Hurwitz if and only if all the matrices $\mathbf{A}$-$c\,\lambda_i\,\mathbf{B}K$, $\forall i \in \{1,2,\ldots,\text{N}\}$ are Hurwitz.

*Lemma 2* [35]. Let ($\mathbf{A}$,$\mathbf{B}$) be stabilizable and matrices $Q$=$Q^T$ and $R$=$R^T$ be positive definite. Let feedback gain $K$ be chosen as

$$K = R^{-1}\mathbf{B}^T P_1, \tag{37}$$

where $P_1$ is the unique positive definite solution of the control algebraic Riccati equation (ARE) [34]

$$\mathbf{A}^T P_1 + P_1\mathbf{A} + Q - P_1\mathbf{B}R^{-1}\mathbf{B}^T P_1 = 0. \tag{38}$$

Then, all the matrices $\mathbf{A}$-$c\,\lambda_i\,\mathbf{B}K$, $\forall i \in \{1,2,\ldots,\text{N}\}$ are Hurwitz if $c \geq \frac{1}{2\lambda_{\min}}$, where $\lambda_{\min} = \min_{i\in \text{N}} Re(\lambda_i)$ ( $Re(\lambda_i)$ denotes the real part of $\lambda_i$).

*Theorem.* Let the digraph $Gr$ have a spanning tree and $g_i \neq 0$ for one DG placed on a root node of the digraph $Gr$. It is assumed that the internal dynamics of each DG are asymptotically stable. Let the auxiliary control $v_i$ in (28) be

$$v_i = -cK\mathbf{e}_i, \tag{39}$$

where $c \in R$ is the coupling gain, and $K \in R^{1\times 2}$ is the feedback control vector. Then, all $\mathbf{y}_i$ in (30) synchronize to $\mathbf{y}_0$ in (31) and, hence, the direct term of DG output voltages $v_{odi}$ synchronizes to $v_{ref}$, if $K$ is chosen as in (37) and

$$c \geq \frac{1}{2\lambda_{\min}}, \tag{40}$$

where $\lambda_{\min} = \min_{i\in \text{N}} Re(\lambda_i)$.

*Proof :* Consider the Lyapunov function candidate

$$V = \frac{1}{2}\boldsymbol{\delta}^T P_2 \boldsymbol{\delta}, \quad P_2 = P_2^T,\ P_2 > 0, \tag{41}$$

where $\boldsymbol{\delta}$ is the global disagreement vector in (33). Then

$$\begin{aligned} \dot{V} &= \boldsymbol{\delta}^T P_2 \dot{\boldsymbol{\delta}} = \boldsymbol{\delta}^T P_2 \left(\dot{\mathbf{Y}} - \dot{\mathbf{Y}}_0\right) \\ &= \boldsymbol{\delta}^T P_2 \left((I_N \otimes \mathbf{A})\boldsymbol{\delta} + (I_N \otimes \mathbf{B})\mathbf{v}\right). \end{aligned} \tag{42}$$

The global auxiliary control $\mathbf{v}$ can be written as

$$\mathbf{v} = -c(I_N \otimes K)\big((L+G)\otimes I_2\big)\boldsymbol{\delta}. \tag{43}$$

Placing (43) into (42) yields

$$\dot{V} = \boldsymbol{\delta}^T P_2 \left(I_N \otimes \mathbf{A} - c(L+G)\otimes \mathbf{B}K\right)\boldsymbol{\delta} \equiv \boldsymbol{\delta}^T P_2 \mathbf{H}\boldsymbol{\delta}. \tag{44}$$

From Lemma 1 and Lemma 2, $\mathbf{H}$ is Hurwitz. Therefore, given any positive real number $\beta$, the positive definite matrix $P_2$ can be chosen such that the following Lyapunov equation holds,

$$P_2\mathbf{H} + \mathbf{H}^T P_2 = -\beta I_{2N}, \tag{45}$$

Placing (45) in (44) yields

$$\dot{V} = \boldsymbol{\delta}^T P_2 \mathbf{H}\boldsymbol{\delta} = \frac{1}{2}\boldsymbol{\delta}^T (P_2\mathbf{H} + \mathbf{H}^T P_2)\boldsymbol{\delta} = -\frac{\beta}{2}\boldsymbol{\delta}^T I_{2N}\boldsymbol{\delta}. \tag{46}$$

Equation (46) shows that $\dot{V} \leq 0$. Therefore, the global disagreement vector $\boldsymbol{\delta}$, (27), and (39) are asymptotically stable and all $\mathbf{y}_i$ in (30) synchronize to $\mathbf{y}_0$ in (31). Hence the direct term of DG output voltages $v_{odi}$ synchronizes to $v_{ref}$. If the internal dynamics are asymptotically stable, then they are all bounded. This completes the proof. □

The block diagram of secondary voltage control based on distributed cooperative control is shown in Fig. 5. As seen, the

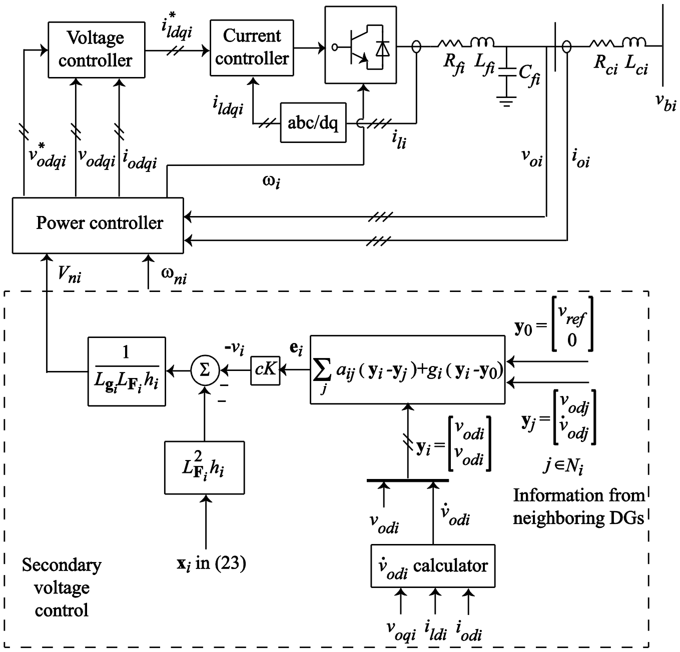

Fig. 5. The block diagram of the proposed secondary voltage control.

control input $V_{ni}$ is implemented using (28). Each DG has a $\dot{v}_{odi}$ calculator block based on (17).

Choosing the coupling gain $c$ and the feedback control vector $K$ based on (37) and (40) ensures the asymptotic stability of the controller. Moreover, these controller parameters can adjust the response speed of the secondary voltage control.

### *C. The Required Sparse Communication Topology for Secondary Control*

The proposed secondary voltage control must be supported by a local communication network that provides its required information flows. This communication graph should be designed to reduce transmission delays and the required information flows between components. Long communication links are not desired [19]. For the microgrids with a small geographical span, the communication network can be implemented by CAN Bus and PROFIBUS communication protocols [12], [36]. It should be noted that communication links contain an intrinsic delay. However, in this paper, the communication link delays are assumed to be zero. Since the time scale of the secondary control is large enough, the aforementioned assumption is valid and the communication link delays do not significantly affect the system performance [12].

According to the results of the theorem in Section IV.B, the communication topology should be a graph containing a spanning tree in which the secondary control of each DG only requires information about that DG and its immediate neighbors in the communication graph. Therefore, the communication requirements for implementing the proposed control are rather mild. Given the physical structure of the microgrid, it is not difficult to select a graph with a spanning tree that connects all the DGs in an optimal fashion. Such optimal connecting graphs can be designed using operations research or assignment problem solutions [37]-[38]. The optimization criteria can include minimal lengths of the communication links, maximal use of existing communication links, minimal number of links, and etc.

## V. Case Studies

The effectiveness of the proposed secondary voltage control is verified by simulating an islanded microgrid in Matlab. Figure 6 illustrates the single line diagram of the microgrid test system. This microgrid consists of four DGs. The lines between buses are modeled as series RL branches. The specifications of the DGs, lines, and loads are summarized in Table 1.

It is assumed that DGs communicate with each other through the communication digraph depicted in Fig. 7. This communication topology is chosen based on the geographical location of DGs. The associated adjacency matrix of the digraph in Fig. 7 is

$$A_G = \begin{bmatrix} 0 & 0 & 0 & 0 \\ 1 & 0 & 0 & 0 \\ 0 & 1 & 0 & 0 \\ 1 & 0 & 0 & 0 \end{bmatrix}. \tag{47}$$

DG 1 is the only DG that is connected to the leader node with the pinning gain $g_1$=1.

In the following, first, the effectiveness of the proposed secondary voltage control is shown for three different reference voltage values. Then, the effects of the algebraic Riccati equation parameters on the transient response of the controller are studied.

### *A. Simulation Results for Different Reference Voltage Values*

In this section, the coupling gain in (39) is $c$=4 which satisfies (40). The solution of the algebraic Riccati equation in (38) is used to calculate the feedback control vector $K$ in (39).

TABLE I

SPECIFICATIONS OF THE MICROGRID TEST SYSTEM

| | | | | | | |
|---|---|---|---|---|---|---|
| | DG 1 & 2 (45 kVA rating) | | DG 3 & 4 (34 kVA rating) | | | |
| DGs | $m_P$ | $9.4\times10^{-5}$ | $m_P$ | $12.5\times10^{-5}$ | | |
| | $n_Q$ | $1.3\times10^{-3}$ | $n_Q$ | $1.5\times10^{-3}$ | | |
| | $R_c$ | 0.03 Ω | $R_c$ | 0.03 Ω | | |
| | $L_c$ | 0.35 mH | $L_c$ | 0.35 mH | | |
| | $R_f$ | 0.1 Ω | $R_f$ | 0.1 Ω | | |
| | $L_f$ | 1.35 mH | $L_f$ | 1.35 mH | | |
| | $C_f$ | 50 µF | $C_f$ | 50 µF | | |
| | $K_{PV}$ | 0.1 | $K_{PV}$ | 0.05 | | |
| | $K_{IV}$ | 420 | $K_{IV}$ | 390 | | |
| | $K_{PC}$ | 15 | $K_{PC}$ | 10.5 | | |
| | $K_{IC}$ | 20000 | $K_{IC}$ | 16000 | | |
| | Line 1 | | Line 2 | | Line 3 | |
| Lines | $R_{l1}$ | 0.23 Ω | $R_{l2}$ | 0.35 Ω | $R_{l3}$ | 0.23 Ω |
| | $L_{l1}$ | 318 µH | $L_{l2}$ | 1847 µH | $L_{l3}$ | 318 µH |
| | Load 1 | | Load 2 | | | |
| Loads | $P_{L1}$ (per phase) | 12 kW | $P_{L2}$ (per phase) | 15.3 kW | | |
| | $Q_{L1}$ (per phase) | 12 kVAr | $Q_{L2}$ (per phase) | 7.6 kVAr | | |

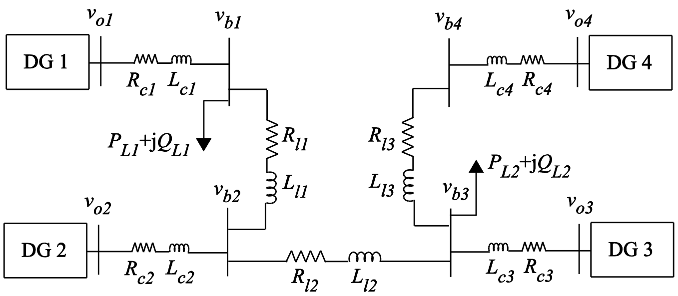


Fig. 6. Single line diagram of the microgrid test system.

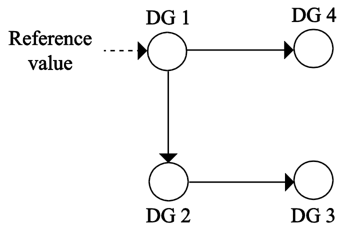


Fig. 7. Topology of the communication digraph.

In (38), the algebraic Riccati equation parameters are chosen as $Q=\begin{bmatrix}50000 & 0\\ 0 & 1\end{bmatrix}$ and $R$=0.01. The resulting feedback control vector is $K$=[2236 67.6].

In the first case, namely *Case A*, the microgird is islanded from the main grid at $t$=0, while the secondary control is active. Figures 8a, 8b, and 8c show the DG terminal voltage amplitudes when the reference voltage value is set to 1 pu, 0.95 pu, and 1.05 pu, respectively. As seen in Fig. 8, the secondary control returns all DG terminal voltage amplitudes to the pre-specified reference values after 0.1 seconds.

It should be noted that the secondary control level always exists as a supervisory control level and take actions in the event of disturbances. However, to highlight the effectiveness of the proposed secondary control, a new case study, namely *Case B*, is considered. It is assumed that the microgrid is islanded from the main grid at $t$=0, and the secondary control is applied at $t$=0.6 s. Figures 9a, 9b, and 9c show the simulation results when the reference voltage value is set to 1 pu, 0.95 pu, and 1.05 pu, respectively. As seen in Fig. 9, while the primary control keeps the voltage amplitudes stable, the secondary control returns all terminal voltage amplitudes to the pre-specified reference values after 0.1 seconds.

*B. The Effect of Algebraic Riccati Equation (ARE) Parameters on the Transient Response*

The ARE parameters have a direct impact on the transient response of the proposed secondary voltage control. The ARE in (38) is extracted by minimizing the following performance index for each DG [34]

$$J_i=\frac{1}{2}\int_0^{\infty}(\boldsymbol{\delta}_i^T Q\boldsymbol{\delta}_i+v_i^T R v_i)dt, \tag{48}$$

where the local disagreement vector is

$$\boldsymbol{\delta}_i=\mathbf{y}_i-\mathbf{y}_0. \tag{49}$$

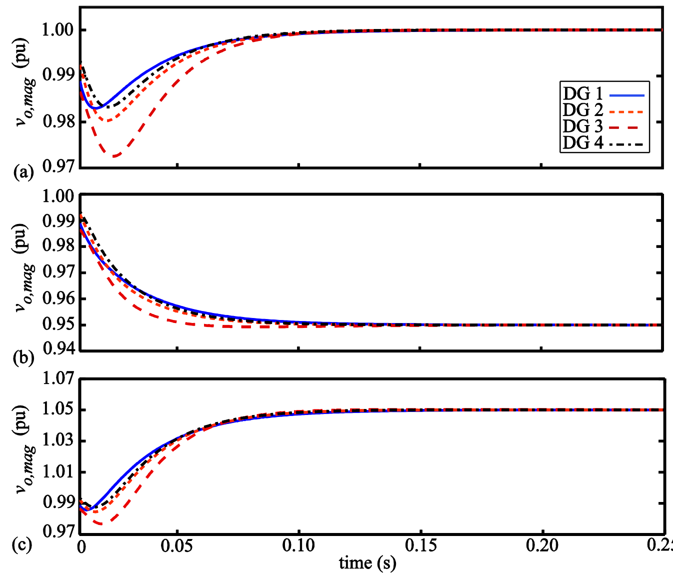


Fig. 8. DG output voltage magnitudes for *Case A*: (a) when $v_{ref}$=1 pu, (b) when $v_{ref}$=0.95 pu, and (c) when $v_{ref}$=1.05 pu.

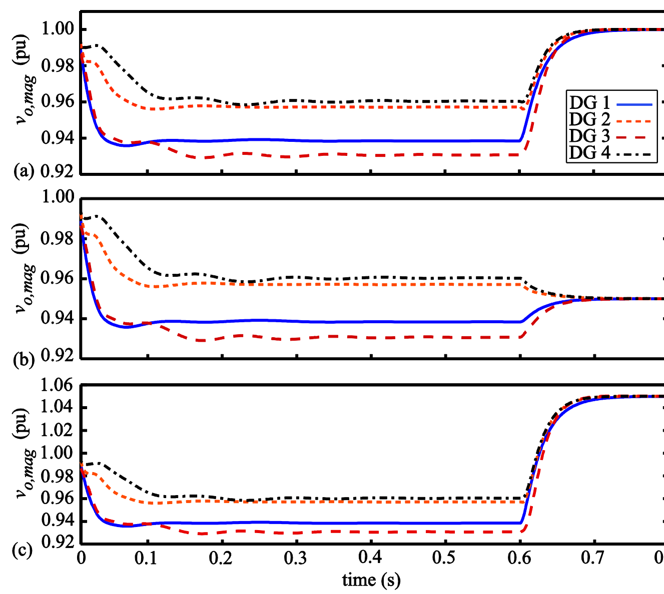


Fig. 9. DG output voltage magnitudes for *Case B*: (a) when $v_{ref}$=1 pu, (b) when $v_{ref}$=0.95 pu, and (c) when $v_{ref}$=1.05 pu.

The performance index $J_i$ can be interpreted as an energy function and the controller is designed to make it as small as possible. The ARE parameters $Q$ and $R$ directly influence the transient response of the controller. Generally speaking, a larger $Q$ means that $\boldsymbol{\delta}_i$ is kept smaller by the controller for keeping $J$ small. On the other hand, a larger $R$ means that $v_i(t)$ is kept smaller by the controller for keeping $J$ small. Therefore, larger $Q$ or smaller $R$ generally result in the poles of the closed-loop system matrix to move left in the s-plane so that the system response speed increases.

To show the effect of the ARE parameters on the response speed of the secondary voltage control, two different cases are considered. The reference value for the terminal voltage of DGs is set to 1 pu. In the first case, ARE parameters are set as $Q=\begin{bmatrix}1000 & 0\\ 0 & 1\end{bmatrix}$ and $R=0.01$. Compared with the case

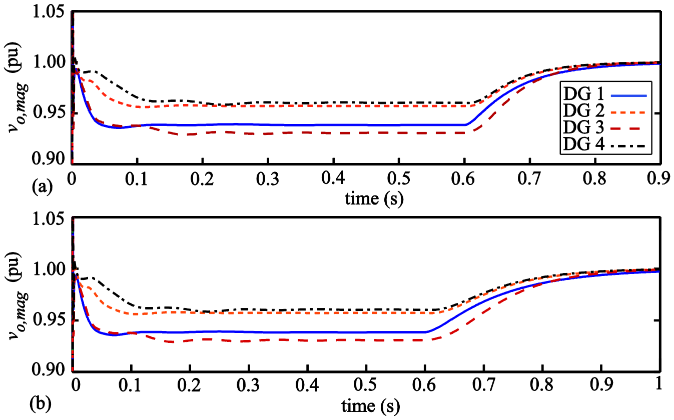


Fig. 10. DG output voltage magnitudes with the following control parameters: (a) $Q=\begin{bmatrix}1000 & 0\\ 0 & 1\end{bmatrix}$ and $R=0.01$, and (b) $Q=\begin{bmatrix}50000 & 0\\ 0 & 1\end{bmatrix}$ and $R=5$.

studied in Fig. 8a, the element in the first row and column of matrix $Q$, which directly affects the control of $v_{odi}$, is smaller. Figure 10a shows the DG output voltage magnitudes before and after applying the secondary control. As seen, the terminal voltage amplitudes synchronize to 1 pu after 0.2 s. Therefore, with a smaller $Q$, the secondary voltage control is slower than the case studied in Fig. 8a.

In the second case, the ARE parameters are set as $Q=\begin{bmatrix}50000 & 0\\ 0 & 1\end{bmatrix}$ and $R=5$. Compared with the case studied in Fig. 8a, $R$ is larger. Figure 10b shows the DG output voltage magnitudes before and after applying the secondary control. As seen, the terminal voltage amplitudes converge to 1 pu after 0.4 s. Therefore, with a larger $R$, the secondary voltage control is slower than the case studied in Fig. 8a.

## VI. Conclusion

In this paper, the concept of distributed cooperative control of multi-agent systems is adopted to implement the secondary voltage control of microgrids. Input-output feedback linearization is used to transform the nonlinear dynamics of DGs to linear dynamics. Feedback linearization converts the secondary voltage control to a second-order tracker synchronization problem. The controller for each DG is fully distributed. Each DG only requires its own information and the information of some neighbors. The proposed microgrid secondary control requires a sparse communication network with one-way communication links and is more reliable than centralized secondary controls. It is shown that the controller parameters can effectively tune the controller synchronization speed.

## References


[1] B. Fahimi, A. Kwasinski, A. Davoudi, R. S. Balog, and M. Kiani, “Charge it,” *IEEE Power & Energy Magazine*, vol. 9, pp. 54-64, July/Aug. 2011.

[2] A. Mehrizi-sani and R. Iravani, “Online setpoint adjustment for trajectory shaping in microgrid applications,” *IEEE Trans. Power Syst.*, vol. 27, pp. 216-223, Feb. 2012.

[3] A. Bidram, M. E. Hamedani-golshan, and A. Davoudi, “Capacitor design considering first swing stability of distributed generations,” *IEEE Trans. Power Syst.*, vol. 27, pp. 1941-1948, Nov. 2012.

[4] R. H. Lasseter, “Microgrid,” in *Proc. IEEE Power Eng. Soc. Winter Meeting*, vol. 1, New York, 2002, pp. 305-308.

[5] J. M. Guerrero, M. Chandorkar, T. L. Lee, and P. C. Loh, “Advanced control artchitectures for intelligent microgrids-Part I: Decentralized and hierarchical control,” *IEEE Trans. Ind. Electron.*, vol. 60, pp. 1254-1262, April. 2013.

[6] J. M. Guerrero, J. C. Vásquez, J. Matas, M. Castilla, L. G. d. Vicuña, and M. Castilla, “Hierarchical control of droop-controlled AC and DC microgrids-A general approach toward standardization,” *IEEE Trans. Ind. Electron.*, vol. 58, pp. 158-172, Jan. 2011.

[7] A. Bidram and A. Davoudi, “Hierarchical structure of microgrids control system,” *IEEE Trans. Smart Grid*, vol. 3, pp. 1963-1976, Dec. 2012.

[8] G. Diaz, C. Gonzalez-Moran, J. Gomez-Aleixandre, and A. Diez, “Scheduling of droop coefficients for frequency and voltage regulation in isolated microgrids,” *IEEE Trans. Power Syst.*, vol. 25, pp. 489-496, Feb. 2010.

[9] C. K. Sao and W. Lehn, “Control and power management of converter fed microgrids,” *IEEE Trans. Power Syst.*, vol. 23, pp. 1088-1098, Aug. 2008.

[10] P. H. Divshali, A. Alimardani, S. H. Hosseinian, and M. Abedi, “Decentralized cooperative control strategy of microsources for stabilizing autonomous VSC-based microgrids,” *IEEE Trans. Power Syst.*, vol. 27, pp. 1949-1959, Nov. 2012.

[11] M. D. Ilic and S. X. Liu, *Hierarchical power systems control: Its value in a changing industry*. London, U.K.: Springer, 1996.

[12] A. Mehrizi-Sani and R. Iravani, “Potential-function based control of a microgrid in islanded and grid-connected models,” *IEEE Trans. Power Syst.*, vol. 25, pp. 1883-1891, Nov. 2010.

[13] J. A. P. Lopes, C. L. Moreira, and A. G. Madureira, “Defining control strategies for microgrids islanded operation,” *IEEE Trans. Power Syst.*, vol. 21, pp. 916-924, May 2006.

[14] F. Katiraei, M. R. Iravani, and P. W. Lehn, “Microgrid autonomous operation during and subsequent to islanding process,” *IEEE Trans. Power Del.*, vol. 20, pp. 248-257, Jan. 2005.

[15] M. Savaghebi, A. Jalilian, J. Vasquez, and J. Guerrero, “Secondary control scheme for voltage unbalance compensation in an islanded droop-controlled microgrid,” *IEEE Trans. Smart Grid*, vol. 3, pp. 797-807, June 2012.

[16] M. Savaghebi, A. Jalilian, J. Vasquez, and J. Guerrero, “Secondary control for voltage quality enhancement in microgrids,” *IEEE Trans. Smart Grid*, vol. 3, pp. 1893-1902, Dec. 2012.

[17] F. Katiraei and M. R. Iravani, “Power management strategies for a microgrid with multiple distributed generation units,” *IEEE Trans. Power Syst.*, vol. 21, pp.1821-1831, Jan. 2005.

[18] B. Marinescu and H. Bourles, “Robust predictive control for the flexible coordinated secondary voltage control of large scale power system,” *IEEE Trans. Power Syst.*, vol. 14, pp. 1262-1268, Nov. 1999.

[19] H. Xin, Z. Qu, J. Seuss, and A. Maknouninejad, “A self-organizing strategy for power flow control of photovoltaic generators in a distribution network,” *IEEE Trans. Power Syst.*, vol. 26, pp. 1462-1473, Aug. 2011.

[20] S. D. J. McArthur, E. M. Davidson, V. M. Catterson, A. L. Dimeas, N. D. Hatziargyriou, F. Ponci, and T. Funabashi, “Multi-agent systems for power engineering applications-part I: Concepts, approaches, and technical challenges,” *IEEE Trans. Power Syst.*, vol. 22, pp. 1743-1752, Nov. 2007.

[21] Q. Hui and W. Haddad, “Distributed nonlinear control algorithms for network consensus,” *Automatica*, vol. 42, pp. 2375–2381, 2008.

[22] J. Fax and R. Murray, “Information flow and cooperative control of vehicle formations,” *IEEE Trans. Automatic Control*, vol. 49, pp. 1465–1476, Sept. 2004.

[23] W. Ren and R. W. Beard, *Distributed consensus in multi-vehicle cooperative control*. Berlin: Springer, 2008.

[24] Z. Qu, *Cooperative control of dynamical systems: Applications to autonomous vehicles*. New York: Springer-Verlag, 2009.

[25] A. Jadbabaie, J. Lin, and A. S. Morse, “Coordination of groups of mobile autonomous agents using nearest neighbor rules,” *IEEE Trans. Automatic Control*, vol. 48, pp. 988–1001, June 2003.

[26] X. Li, X. Wang, and G. Chen, “Pinning a complex dynamical network to its equilibrium,” *IEEE Trans. Circuits and Systems I: Regular Papers*, vol. 51, 2074–2087, Oct. 2004.

[27] Z. Li, Z. Duan, G. Chen, and L. Huang, “Consensus of multi-agent systems and synchronization of complex networks: a unified viewpoint,” *IEEE Trans. Circuits and Systems I*, vol. 57, pp. 213–224, Jan. 2010.

[28] A. Das and F. L. Lewis, "Distributed adaptive control for synchronization of unknown nonlinear networked systems," *Automatica*, vol. 46, pp. 2014-2021, 2010.
[29] N. Pogaku, M. Prodanovic, and T. C. Green, "Modeling, analysis and testing of autonomous operation of an inverter-based microgrid," *IEEE Trans. Power Electron.*, vol. 22, pp. 613–625, March 2007.
[30] M. N. Marwali and A. Keyhani, "Control of distributed generation systems part I: Voltage and currents control," *IEEE Trans. Power Electron.*, vol. 19, pp. 1541–1550, Nov. 2004.
[31] A. Keyhani, M. N. Marwali, and M. Dai, *Integration of green and renewable energy in electric power systems*. New Jersey: Wiley, 2010.
[32] J. J. E. Slotine and W. Li, *Applied nonlinear control*. New Jersey: Prentice-Hall, 2009.
[33] J. W. Brewer, "Kronecker products and matrix calculus in system theory," *IEEE Trans. Circuits and Systems*, vol. 25, pp. 772-781, Sept. 1978.
[34] F. L. Lewis and V. L. Syrmos, *Optimal control*. New York: Wiley, 1995.
[35] H. Zhang, F. L. Lewis, and A. Das, "Optimal design for synchronization of cooperative systems: State feedback, observer, and output feedback," *IEEE Trans. Automatic Control*, vol. 56, pp. 1948–1952, Aug. 2011.
[36] E. Bassi, F. Benzi, L. Lusetti, and G. S. Buja, "Communication protocols for electrical drives," in *Proc. 21st Int. Conf. Industrial Electronics (IECON)*, 1995, pp. 706–711.
[37] R. K. Ahuja, T. L. Magnanti, and J. B. Orlin, *Network flows: theory, algorithms, and applications*. Englewood Cliffs: Prentice Hall: 1993.
[38] R. Burkard, M. Dell'Amico, and S. Martello, *Assignment Problems*. Philadelphia: SIAM: 2009.


**Ali Bidram** (S'09) received the B.S. (Hon.) and M.S. (Hon.) degree in electrical engineering from Isfahan University of Technology, Isfahan, Iran, in 2008 and 2010, respectively. He is currently pursuing the Ph.D. degree at the University of Texas at Arlington, Arlington, TX. His research interests include power system dynamics, distributed control systems, micro-grid, and renewable energy resources.

**Ali Davoudi** (S'04, M'11) is currently an Assistant Professor at the Electrical Engineering department of the University of Texas at Arlington. He received his Ph. D. in Electrical and Computer Engineering from the University of Illinois, Urbana-Champaign, USA, in 2010. He received B.Sc. and M.Sc. degrees in Electrical and Computer Engineering from Sharif University of Technology, Tehran, Iran, and The University of British Columbia, Vancouver, Canada, in 2003 and 2005, respectively. He worked for Solar Bridge Technologies, Texas Instruments Inc., and Royal Philips Electronics. He is an Associate Editor for IEEE Transactions on Vehicular Technology, IEEE Transactions on Industry Applications, and IEEE Transactions on Industrial Informatics. He is also a Guest Associate Editor for IEEE Transactions on Power Electronics, special issue on Transportation Electrification and Vehicle Systems. His research interests are various aspects of modeling, simulation, and control of power electronics, energy conversion systems, and finite-inertia power systems.

**Frank L. Lewis** (S'78–M'81–SM'86–F'94) obtained the bachelor's degree in physics/EE and the MSEE at Rice University, Houston, TX, the M.S. degree in aeronautical engineering from University of West Florida, Pensacola, and the Ph.D. degree at Georgia Institute of Technology, Atlanta. He works in feedback control, intelligent systems, distributed control systems, and sensor networks. He is author of 6 U.S. patents, 216 journal papers, 330 conference papers, 14 books, 44 chapters, and 11 journal special issues. Dr. Lewis is a Fellow of IFAC and the U.K. Institute of Measurement and Control, a PE in Texas, and a U.K. Chartered Engineer. He is also a Distinguished Scholar Professor and Moncrief-O'Donnell Chair at University of Texas at Arlington's Research Institute. He received the Fulbright Research Award, NSF Research Initiation Grant, ASEE *Terman Award*, Int. Neural Network Soc. *Gabor Award* 2009, and the U.K. Institute of Measurement & Control *Honeywell Field Engineering Medal* 2009. 2012 *Neural Networks Pioneer Award* from IEEE CIS. He received Outstanding Service Award from Dallas IEEE Section, was selected as Engineer of the Year by Ft. Worth IEEE Section, was listed in Ft. Worth Business Press Top 200 Leaders in Manufacturing, received the 2010 IEEE Region 5 Outstanding Engineering Educator Award and the 2010 UTA Graduate Dean's Excellence in Doctoral Mentoring Award, and has served on the NAE Committee on Space Station in 1995. He is an elected Guest Consulting Professor at South China University of Technology, Guangzhou, China, and Shanghai Jiao Tong University, Shanghai. He is a Founding Member of the Board of Governors of the Mediterranean Control Association.

**Josep M. Guerrero** (S'01-M'04-SM'08) received the B.S. degree in telecommunications engineering, the M.S. degree in electronics engineering, and the Ph.D. degree in power electronics from the Technical University of Catalonia, Barcelona, in 1997, 2000 and 2003, respectively. He was an Associate Professor with the Department of Automatic Control Systems and Computer Engineering, Technical University of Catalonia, teaching courses on digital signal processing, field-programmable gate arrays, microprocessors, and control of renewable energy. In 2004, he was responsible for the Renewable Energy Laboratory, Escola Industrial de Barcelona. Since 2011, he has been a Full Professor with the Department of Energy Technology, Aalborg University, Aalborg East, Denmark, where he is responsible for the microgrid research program. From 2012 he is also a guest Professor at the Chinese Academy of Science and the Nanjing University of Aeronautics and Astronautics. His research interests is oriented to different microgrid aspects, including power electronics, distributed energy-storage systems, hierarchical and cooperative control, energy management systems, and optimization of microgrids and islanded minigrids. Prof. Guerrero is an Associate Editor for the IEEE TRANSACTIONS ON POWER ELECTRONICS, the IEEE TRANSACTIONS ON INDUSTRIAL ELECTRONICS, and the IEEE Industrial Electronics Magazine. He has been Guest Editor of the IEEE TRANSACTIONS ON POWER ELECTRONICS Special Issues: Power Electronics for Wind Energy Conversion and Power Electronics for Microgrids, and the IEEE TRANSACTIONS ON INDUSTRIAL ELECTRONICS Special Sections: Uninterruptible Power Supplies systems, Renewable Energy Systems, Distributed Generation and Microgrids, and Industrial Applications and Implementation Issues of the Kalman Filter. He currently chairs the Renewable Energy Systems Technical Committee of the IEEE Industrial Electronics Society.